The Nature of Persistent Conformational Chirality, Racemization Mechanisms, and Predictions in Diarylether Heptanoid Cyclophane Natural Products

Citation	Pattawong, O., Salih, M. Q., Rosson, N. T., Beaudry, C. M., & Cheong, P. H. Y. (2014). The nature of persistent conformational chirality, racemization mechanisms, and predictions in diarylether heptanoid cyclophane natural products. Organic & Biomolecular Chemistry, 12(20), 3303-3309. doi:10.1039/c3ob42550a
DOI	10.1039/c3ob42550a
Publisher	Royal Society of Chemistry
Version	Accepted Manuscript
Terms of Use	http://cdss.library.oregonstate.edu/sa-termsofuse

Journal Name

Dynamic Article Links ▶

Cite this: DOI: 10.1039/c0xx00000x

www.rsc.org/xxxxxx

ARTICLE TYPE

The Nature of Persistent Conformational Chirality, Racemization Mechanisms, and Predictions in Diarylether Heptanoid Cyclophane Natural Products†

Ommidala Pattawong, M. Quamar Salih, Nicholas T. Rosson, Christopher M. Beaudry* and Paul Ha-Yeon Cheong*

Received (in XXX, XXX) Xth XXXXXXXXX 20XX, Accepted Xth XXXXXXXXX 20XX
DOI: 10.1039/b000000x

Restricted rotations of chemical bonds can lead to the presence of persistent conformational chirality in molecules lacking stereocenters. We report the development of first-of-a-kind predictive rules that enable identification of conformational chirality and prediction of racemization barriers in the diarylether heptanoid (DAEH) natural products that do not possess stereocenters. These empirical rules-of-thumb are based on quantum mechanical computations (SCS-MP2/∞//B3LYP/6-31G*/PCM) of racemization barriers of four representative DAEHs. Specifically, the local symmetry of ring B and the *E/Z* configuration of the vinylogous acid/ester are critical in determining conformational chirality in the DAEH natural product family.

Molecular chirality is of paramount importance to chemistry, biology, and medicine.[1] Small molecules that are chiral by virtue of restricted rotations (atropisomerism), or conformational chirality, are an underdeveloped territory with the potential for new developments of chiral ligands, medicinal compounds, catalysts, and materials. At present, there are no known methods to predict the presence of persistent conformational chirality in these compounds based solely on their molecular architecture without resorting to total synthesis.[2,3] Specifically in this report, we have developed predictive rules-of-thumb for the chiral properties of all members in a family of cyclophane natural products called the diarylether heptanoids (DAEHs). Additionally, we elucidate the atomistic and energetic details related to the racemizations.

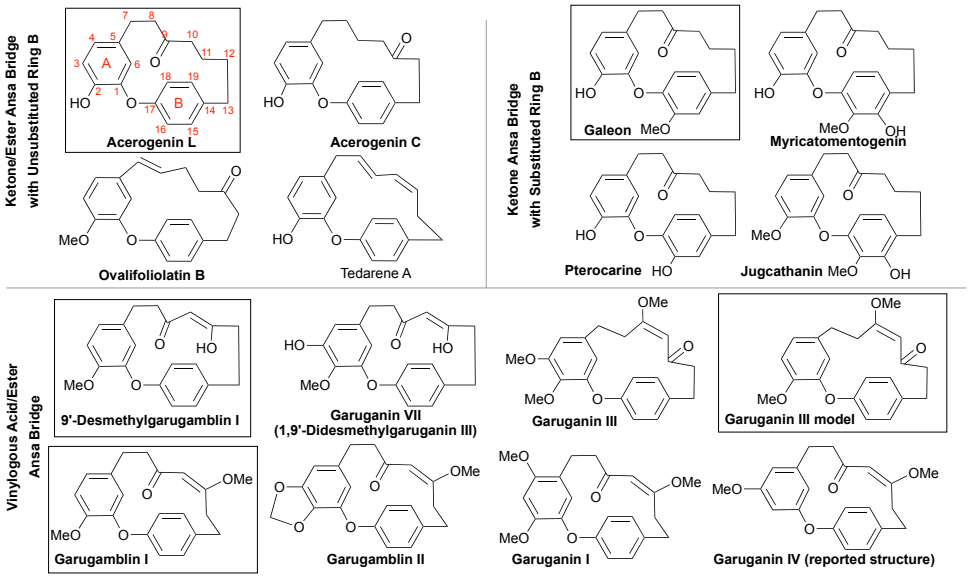

Figure 1. All members in the family of diarylether heptanoids (DAEHs). The five representative DAEHs studied are in boxes.

DAEHs are characterized by oxa[1.7]metaparacyclophane molecular architecture (Figure 1).[4] We (CMB and MQS) recently prepared the DAEHs that lack stereocenters and showed that some (but not all) are chiral.[5] To the best of our knowledge, the presence of conformational chirality in these natural products cannot be predicted without resorting to total synthesis. In addition, determining the mechanism of racemization proved to be challenging even with the natural compound in hand. We

believed that we could address both challenges through computations of four model DAEHs. The four model DAEHs are expected to be representative of similar members of the family because DAEHs that have similar structure type (e.g. the vinylogous acids) were found experimentally to have nearly identical racemization barriers.

We discovered that the complete stereoisomerization of a DAEH requires torsional rotations of all the stereogenic functional groups. The number of possible rotational sequences is equal to the factorial of the number of stereogenic groups in a given DAEH. Therefore, all intermediates and transition structures (TSs) for all possible sequences have been computed for each of the DAEHs discussed at SCS-MP2[6]/def2-∞[7] // B3LYP[8]/6-31G*[9] /PCM (dichlorobenzene)[10] level of theory.[11]

Of four representative DAEHs, acerogenin L most closely resembles the parent DAEH structure. There are two substituents: OH at C_2 and O at C_9. The complete racemization of acerogenin L requires the rotations of 3 stereogenic functional groups: C_7–C_8, C_9O, and C_{11}–C_{12}. There are a total of 3! (6) stereoisomerization pathways for acerogenin L; all were computed (Figure 2, B).

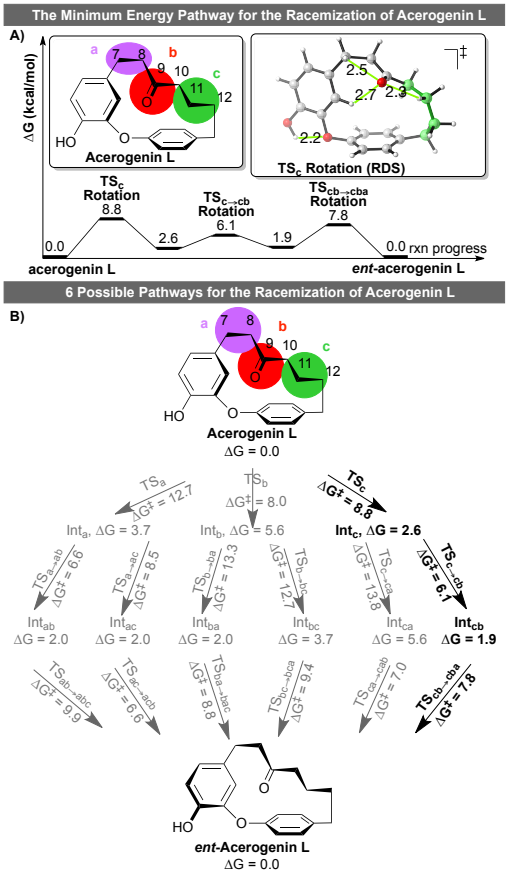

Figure 2.[12,13] A) The minimum energy path and the RDS for racemization of acerogenin L. B) Six possible racemization pathways.

The minimum energy pathway for racemization is shown in Figure 2 (A, B in black). Specifically, the sequence of rotation is: i) C_{11}–C_{12} ($\Delta G^{\ddagger}$ = 8.8 kcal/mol); ii) C_9O ($\Delta G^{\ddagger}$ = 6.1 kcal/mol); iii) C_7–C_8 ($\Delta G^{\ddagger}$ = 7.8 kcal/mol). The rate-determining step (RDS) is the C_{11}–C_{12} rotation with a half-life ($t_{1/2}$) of 3.15 x 10^{-7} s at 25 ºC (in the box, Figure 2). From these barriers, we predict that acerogenin L is achiral – the enantiomeric conformations racemize rapidly under ambient conditions. The experimental racemization barrier measured at –60 ºC is ≤ 10.5 kcal/mol. Consistent with experiments, the predicted barrier at –60 ºC is 8.6 kcal/mol or $t_{1/2}$ = 1.03 x 10^{-4} s.[5]

Galeon differs from acerogenin L by virtue of a C_{16} methoxy substituent. The chiral properties of galeon are representative of all DAEHs with substituents on ring B. This substitution now renders ring B a stereogenic functional group; therefore, there are a total of 4! (24) stereoisomerization pathways for galeon. All 24 racemization pathways for galeon were computed (Figure 3, B).

The minimum energy pathway for racemization is shown in Figure 3 (A, B in black). The racemization of galeon begins with the rotation of the facile rotations of the C_{11}–C_{12}, followed by C_9O and C_7–C_8 functional groups ($\Delta G^{\ddagger}$ = 8.8, 6.6 and 8.7 kcal/mol, respectively), and finally followed by ring B ($\Delta G^{\ddagger}$ = 45.2 kcal/mol at 25 ºC, $t_{1/2}$ = 1.52 x 10^{20} s, RDS). The high computed barrier of ring B rotation suggests that galeon is conformationally chiral under ambient conditions – in fact, the computed barrier at 201 ºC is an enormous 46.4 kcal/mol ($t_{1/2}$ = 1.71 x 10^{8} s). This value agrees with the experimental data ($\Delta G^{\ddagger}$ = 39.6 ± 0.6 kcal/mol).[5]

The large barrier of ring B rotation in galeon ($\Delta G^{\ddagger}$ = 45.2 kcal/mol, Figure 3, A) is due to a gearing mechanism.[14] Specifically, the rotation causes trans-annular strain between aryl hydrogens (H_{18} and H_{19}) and H_6 and H_{11}. It is important to note that the ring B rotational barrier for acerogenin L is identical to that of galeon – the trans-annular strain exists in the rotation of ring B in acerogenin L as well. However, ring B in acerogenin L is symmetric, and the racemization does not require its rotation. Only in galeon, where ring B is substituted, does the racemization require ring B rotation.

We next turned our attention to DAEHs with unsaturation in the ansa chain. It was apparent after consideration of the NMR spectra of these molecules that they have markedly different racemization rates;[5b] however, the nature of these differences was not obvious to us. Specifically, DAEHs with E-configured vinylogous esters racemized slowly on the NMR timescale, but DAEHs with vinylogous acids or Z-configured vinylogous ester racemized quickly on the NMR timescale. Interestingly, 9'-desmethylgarugamblin I, possessing a vinylogous acid in the ansa chain has different ground state geometric preferences compared to garuganin III, with a vinylogous ester ansa chain.

There are a total of five tautomers of 9'-desmethylgarugamblin I (Figure 4): keto, C_9-*E*, C_{11}-*E*, C_9-*Z* and C_{11}-*Z*. The designations C_9 and C_{11} describe the position of the carbonyl, and *Z*/*E* define the stereochemistry of the vinylogous acid. The *Z*- are more stable than the *E*-isomers by ~8–10 kcal/mol, most likely due to the presence of stabilizing H-bonding interaction between the enol and the carbonyl. In fact, our model systems show that almost all the stability differences between the *E*- and the *Z*-tautomers arise from the stability of the intramolecular hydrogen bond in the *Z* (Figure 5). The classical hydrogen bonding interactions present in the *Z*-isomer, is favored over non-classical hydrogen bonding CH···O interactions present in *E-isomers,* by 8.6 kcal/mol.

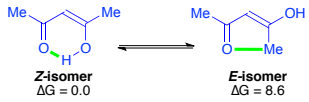

Figure 5.[13] Magnitude of stabilization from the intramolecular hydrogen bonding in 9'-desmethylgarugamblin I

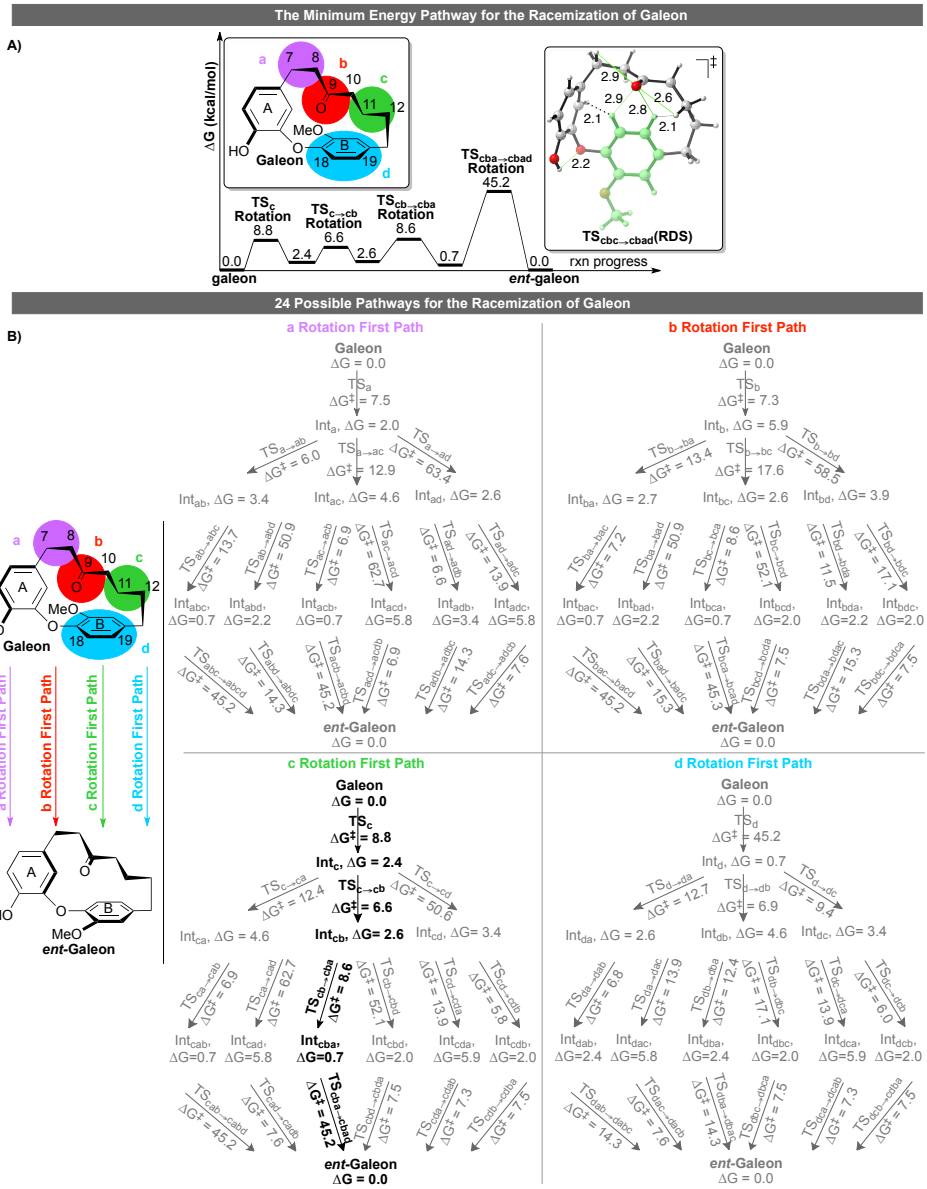

Figure 3.[12,13] A) The minimum energy path and the RDS for racemization of galeon. B) Twenty four possible racemization pathways.

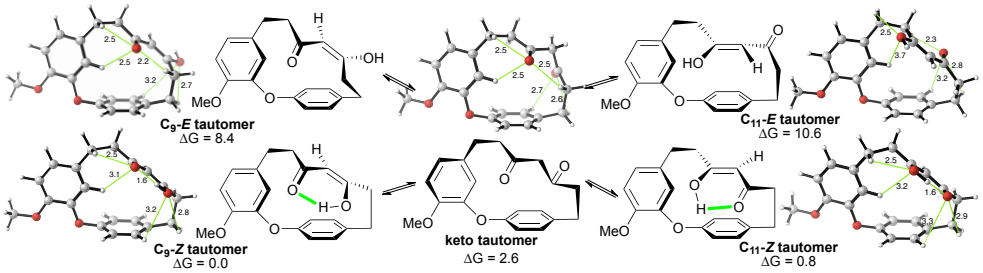

Figure 4.[13b] Five tautomers of 9'-desmethylgarugamblin I.

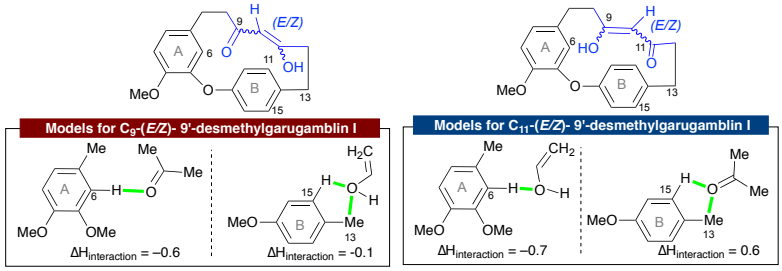

Figure 6. Comparison of strengths of CH···O-ketone/enol interactions, and $C_6H/C_{15}H\cdots O$ interactions found in tautomers of 9'-desmethylgarugamblin I.

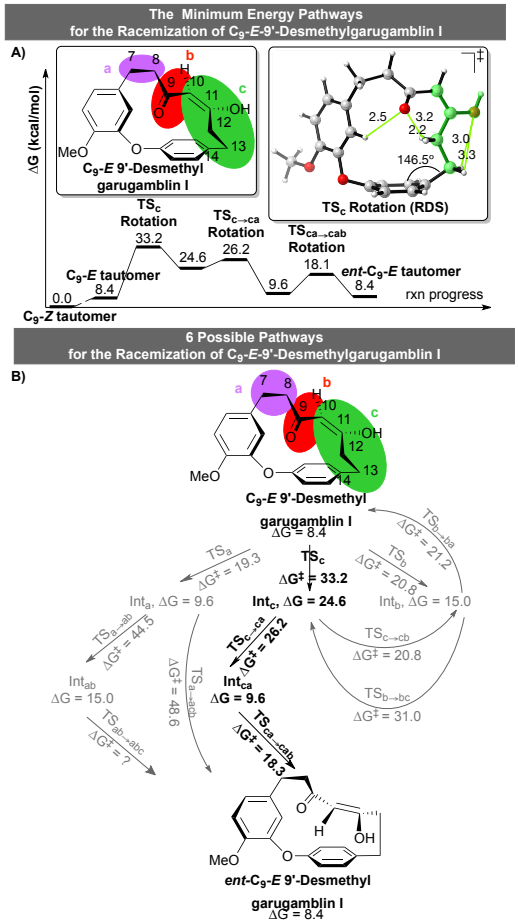

Figure 7.[12,13] A) The minimum energy path and RDS for racemization of C_9-*E*-9`-desmethylgarugamblin I. B) Six possible racemization pathways.

There is a subtle energetic preference for the C_9-regioisomers compared to the C_{11}-regioisomeric vinylogous acid (~1–2 kcal/mol). We originally hypothesized that this is most likely due to the stronger CH···O interactions[15,16] between H_6 and C_9 carbonyl O. Our model system study shows that the ketone oxygen and enol oxygen are similar hydrogen bonding accepters (Figure 6). We thus conclude that the majority of the energetic preference for the C_9/C_{11} arises from subtle conformational and interaction changes from being constrained in a ring.

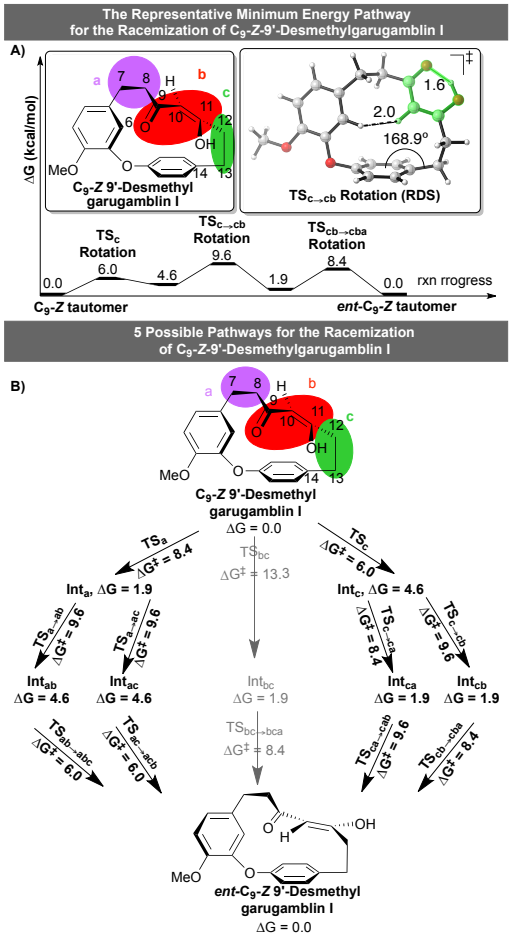

Figure 8.[12,13] A) The representative minimum energy path and RDS for racemization of C_9-*Z*-9`-desmethylgarugamblin I. B) Five possible racemization pathways.

A total of 3! (6) stereoisomerization pathways for the C_9-*E* tautomers of 9'-desmethylgarugamblin I were computed. Surprisingly, only 3 pathways lead to the complete racemization (Figure 7, B). The introduction of an olefin in the ansa chain causes the barrier for functional group rotation to increase dramatically. In particular, $TS_{b\rightarrow ba}$, $TS_{b\rightarrow bc}$ and $TS_{c\rightarrow cb}$ transition states caused the molecule to revert back ($TS_{b\rightarrow ba}$) to the ground state or in the latter cases ($TS_{b\rightarrow bc}$ and $TS_{c\rightarrow cb}$), these led to unproductive isomerization pathways that do not result in racemization due to coupled rotational motions of several functional groups.

The minimum energy pathway for racemization is shown in

Figure 7 (A, B in black). The sequence of rotation is: i) C_{10}-$_{13}$ ($\Delta G^{\ddagger}$ = 33.2 kcal/mol); ii) C_7–C_8 ($\Delta G^{\ddagger}$ = 26.2 kcal/mol); iii) C_9O ($\Delta G^{\ddagger}$ = 18.3 kcal/mol). The rate-determining step (RDS) is the $C_{10\text{-}13}$ rotation with a half-life ($t_{1/2}$) of 2.43 x 10^{11} s at 25 ºC.

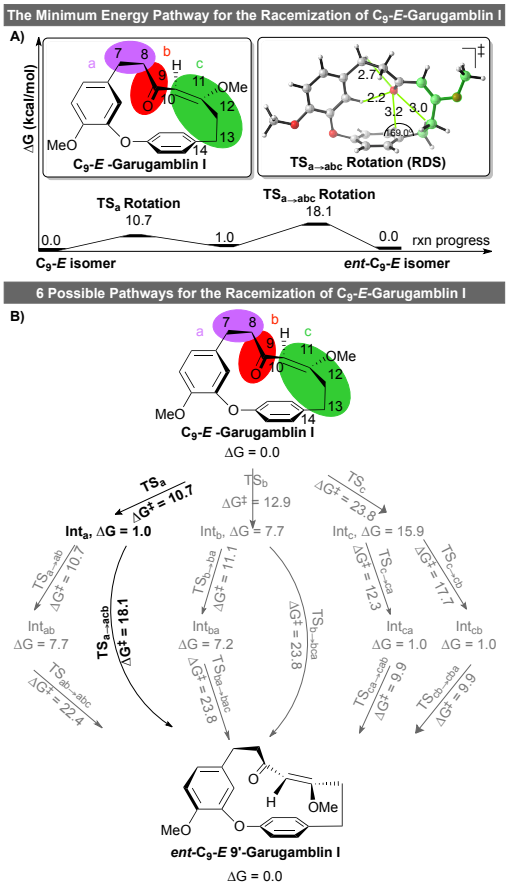

Figure 9.[12,13] A) The minimum energy path and RDS for racemization of C_9-*E*-garugamblin I. B) Six possible racemization pathways.

The complete racemization processes of the more stable C_9-*Z* tautomers of 9'-desmethylgarugamblin I requires the rotations of 3 stereogenic functional groups: C_7–C_8, C_9-C_{10}, and C_{12}–C_{13}. Theoretically, there should be a total of 3! (6) stereoisomerization pathways for C_9-*Z* tautomers. However, computations showed that the process of C_9-C_{10} first rotation is simultaneous with the rotation of C_{12}-C_{13}. Therefore, there are total of five stereoisomerization pathways for C_9-*Z*-9'-desmethylgarugamblin I (Figure 8, B). Interestingly, there are four equivalent minimum energy pathways found for this process (Figure 8, B in black). The representative minimum energy path is shown in Figure 7, A. The rotation of C_{12}-C_{13} is found to be a common RDS for all minimum energy pathways with $\Delta G^{\ddagger}$ = 9.6 kcal/mol or $t_{1/2}$ = 1.22 x 10^{-6} s at 25 ºC. The predicted barrier at -80 ºC is 8.8 kcal/mol, or $t_{1/2}$ = 1.56 x 10^{-3} s. This value agrees well with the experimental data ($\Delta G^{\ddagger}$ = 9.1 kcal/mol or $t_{1/2}$ = 3.3 x 10^{-3} s at -80 ºC).

Surprisingly, the racemization barrier of C_9-*E* tautomer of 9'-desmethylgarugamblin I is higher than the C_9-*Z* by 23.6 kcal/mol (Figures 7 and 8, respectively). In effect, the C_9-*E* vinylogous acids are locked in one regiomeric and diastereomeric conformation and undergo racemization with a higher barrier than the vinylogous acids, which can exist in the C_9-*Z* configuration. This larger barrier comes from the geometric distortions sustained by the macrocycle in the *E*-isomer, as seen by the greater C_{14} out-of-plane distortion in the RDS (146.5º compared to 168.9º).

Since the keto-enol tautomers depicted in Figure 4 are in equilibrium, the molecule will racemize via the reaction coordinate with lowest available transition state. The lowest barrier is the C_9-*Z* tautomer. The calculated barrier corresponds closely with the experimental value.

Lastly, we investigated the vinylogous ester DAEHs. Specifically, garugamblin I and its three vinylogous ester isomers were considered.[17] Again, the designations C_9 and C_{11} describe the position of the carbonyl, and *Z/E* define the stereochemistry of the vinylogous ester. Unlike 9'-desmethylgarugamblin I, the *Z*-stereoisomers of garugamblin I are less stable than the *E* by ~4–6 kcal/mol due to the inherent steric repulsions in the *Z*-vinylogous ester. In fact, the *Z*-conformer is significantly distorted from planarity by ~20º.[17] Similar to the 9'-desmethyl analogue, C_9-*E/Z* tautomers are more stable than C_{11}-*E/Z* tautomers due to stronger CH···O interactions between H_6 and C_9O.

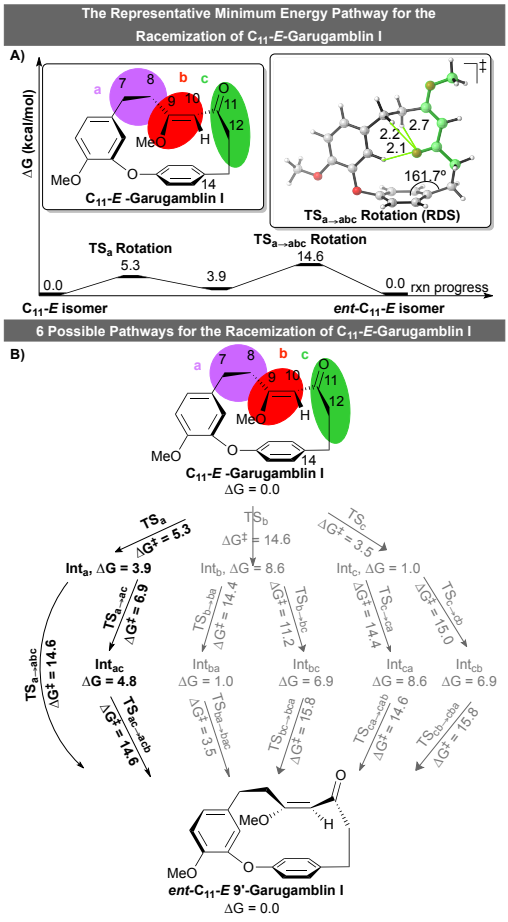

Figure 10.[12,13] A) The representative minimum energy path and RDS for racemization of C_{11}-*E*-garugamblin I. B) Six possible racemization pathways.

All stereoisomerization pathways for the C_9-*Z* and C_9-*E* isomers of garugamblin I were computed. Interestingly, the minimum energy pathway for the racemization of C_9-*E* isomer involves simultaneous rotations of C_9O and $C_{10\text{-}13}$ (Figure 9, B in

black). Consequently, the complete racemization of the C_9-*E* isomer only requires two steps: C_7-C_8 and C_{10-13} rotations. The C_{10-13} rotation is the RDS ($\Delta G^{\ddagger}$ = 18.1 kcal/mol, $t_{1/2}$ = 2.1 s at 25 ºC, Figure 9, A). This value is consistent with the experimental value ($\Delta G^{\ddagger}$ = 16.9 kcal/mol, $t_{1/2}$ = 3.0 x 10^{-1} s at 25 ºC). For the racemization of C_9-*Z* isomer, the vinylogous ester rotation is the RDS ($\Delta G^{\ddagger}$ = 13.8 kcal/mol, $t_{1/2}$ = 1.46 x 10^{-3} s at 25 ºC).[17] We predict that garugamblin I, isolated as the C_9-*E* isomer, would racemize at room temperature on the time scale of seconds.

A total of 3! (6) pathways for complete racemization of C_{11}-*E* tautomer of garugamblin I were computed (Figure 10, B). Two minimum energy pathways are found for this process. The representative of minimum energy pathways is shown in Figure 10, A. Both asynchronous ($TS_{ab\rightarrow abc}$) and synchronous ($TS_{a\rightarrow abc}$) rotations of the vinylogous ester are the RDS with the barrier of 14.6 kcal/mol, or $t_{1/2}$ = 5.63 x 10^{-3} s at 25 ºC (at -10 ºC, $\Delta G^{\ddagger}$ = 14.1, or $t_{1/2}$ = 6.5 x 10^{-2} s). The experimental values for the C_{11}-*E* tautomer of garugamblin I are $\Delta G^{\ddagger}$ = 12.7 kcal/mol, $t_{1/2}$ = 4.4 x 10^{-3} s at –10 ºC. Molecules with this structure type (such as garuganin III) undergo racemization rapidly at room temperature.

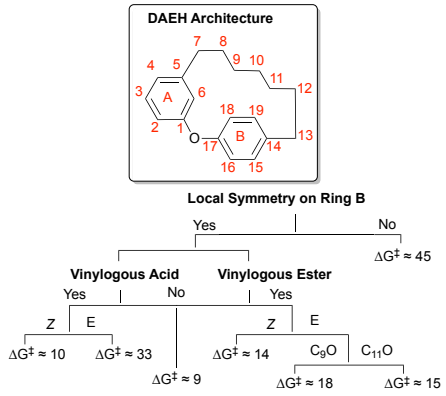

Figure 11.[13b] Predicted barriers for racemization of conformational chirality of the four representative diarylether heptanoids used to deduce the data. $\Delta G^{\ddagger}$ are in kcal/mol.

Conclusions

In conclusion, quantum mechanical computations predict the barriers of racemization for the four representative DAEHs in good agreement with experiments. These have led to the development of a predictive method that enables the identification of persistent conformational chirality and first order rules-of-thumb prediction of racemization barriers of all DAEHs that do not possess stereocenters (Figure 11). The local symmetry of ring B and the *E/Z* configuration of the vinylogous acid/ester are critical in determining molecular conformational chirality in the DAEH natural product family.

Notes and references

Department of Chemistry, Oregon State University, 153 Gilbert Hall, Corvallis, Oregon, 97331-4003, USA.
E-mail: paulc@science.oregonstate.edu, christopher.beaudry@oregonstate.edu; Tel: +1 5417376760

† Electronic Supplementary Information (ESI) available: Coordinates, energies, additional figures, and full authorship of Gaussian. See DOI: 10.1039/b000000x/

1 E. L. Eliel, S. H. Wilen, L. N. Mander, *Stereochemistry of Organic Compounds* WILEY, **1994**.
2 The chiral properties of acyclic diarylethers have been investigated, see: M. S. Betson, J. Clayden, C. P. Worrall, S. Peace, *Angew. Chem. Int. Ed.* **2006,** *45,* 5803-5807.
3 Previously, molecular mechanics computational study of garuganin I using MMP2 forcefield suggested the molecule existed in single enantiomeric conformation at rt. see: Beyer, A.; Kalchhauser, H.; Wolschann, P. *Monatsh. Chem.* 1992, **123,** 417–423. Experimentally, we found this to be inaccurate, see ref. 5b. Computational data presented in this work using quantum mechanics (SCS-MP2/B3LYP) agrees with experimental findings.
4 (a) S. Nagumo, S. Ishizawa, M. Nagai and T. Inoue, *Chem. Pharm. Bull.* 1996, **44**, 1086-1089; (b) K. E. Malterud, T. Anthonsen and J. Hjortas, *Tetrahedron Lett.* 1976, **35**, 3069-3072; (c) J. Zhu, G. Islas–Gonzalez and M. Bois–Choussy, *Org. Prep. Proc. Int.* 2000, **32**, 505-546; (d) P. Claeson, P. Tuchinda and V. Reutrakul, *J. Indian Chem. Soc.* 1994, **71**, 509-521.
5 (a) M. Q. Salih, and C. M. Beaudry, *Org. Lett.* 2012, **14**, 4026–4029; (b) Z.-Q. Zhu, M. Q. Salih, E. Fynn, A. D. Bain, C. M. Beaudry, *J. Org. Chem.* 2013**, 78**, 2881-2896; (c) Z.-Q. Zhu, C. M. Beaudry, *J. Org. Chem.* 2013**, 78**, 3336-3341. (d) M. Q. Salih, C. M. Beaudry, *Org. Lett.* 2013,**15**, 4540-4543. (e) M. Morihara, N. Sakurai, T. Inoue, K.-i. Kawai, M. Nagai, *Chem. Pharm Bull.* 1997, **45**, 820–823.
6 M. Gerenkamp and S. Grimme, *Chem. Phys. Lett.* 2004, **392**, 229.
7 (a) A. Hellweg, C. Hättig, S. Höfener and W. Klopper, *Theor. Chem. Acc.* 2007, **117**, 587; (b) S. Zhong, E. C. Barnes and G. A. Petersson, *J. Chem. Phys.* 2008, **129**, 184116; (c) F. Neese and E. F. Valeev, *J. Chem. Theory Comput.* 2011, **7**, 33.
8 A. D. Becke, *J. Chem. Phys.* 1993, **98**, 5648.
9 (a) W. J. Hehre, R. Ditchfield and J. A. Pople, *J. Chem. Phys.* 1972, **56**, 2257; (b) P. C. Hariharan and J. A. Pople, *Theor. Chim. Acta.* 1973, **28**, 213.
10 (a) PCM: S. Miertuš, E. Scrocco and J. Tomasi, *Chem. Phys.* 1981, **55**, 117; (b) UFF: A. K. Rappé, C. J. Casewit, K. S. Colwell, W. A. Goddard III and W. M. Skiff, *J. Am. Chem. Soc.* 1992, **114**, 10024.
11 This combination of methods has been used for high-accuracy computational studies of organic reactions. (a) O. Pattawong, T. J. L. Mustard, R. C. Johnston, P. H.–Y. Cheong, *Angew. Chem. Int. Ed.* 2013, **52**, 1420. (b) M. D. Pierce, R. C. Johnston, S. Mahapatra, H. Yang, R. G. Carter, P. H.-Y. Cheong, *J. Am. Chem. Soc.* 2012, **134**, 13624. (c) P. G. McGarraugh, R. C. Johnston, A. Martínez-Muñoz, P. H.-Y. Cheong, S. E. Brenner-Moyer, *Chem. Eur. J.* 2012, **18**, 10742–10752. (d) D. Q. Tan, A. Younai, O. Pattawong, J. C. Fettinger, P. H.-Y. Cheong, J. T. Shaw, *Org. Lett.* 2013, **15**, 5126–5129.
12 C. Y. Legault, CYLview 1.0b; UCLA: Los Angeles, CA, 2007.
13 (a) The green highlighted atoms are directly involved in the transition state. Green lines indicate stabilizing hydrogen bonds and CH···O interactions; (b) Distances given in Å, energies in kcal/mol and half-lives in seconds at 25 ºC.
14 C. Rousel, A. Liden, M. Chanon, J. Metzger and J. Sandstrom, *J. Am. Chem. Soc.* 1976, **98**, 2847-2852.
15 (a) R. Hirschmann, Jr. C. S. Snoddy and N. L. Wendler, *J. Am. Chem. Soc.* 1952, **74**, 2693; (b) E. J. Corey, J. J. Rohde, A. Fischer and M. D. Azimioara, *Tetrahedron Lett.* 1997, **38**, 33; (c) B. W. Gung, W. Xue and W. R. Roush, *J. Am. Chem. Soc.* 2002, **124**, 10692; (d) R. S. Paton and J. M. Goodman, *Org. Lett.* 2006, **7**, 4299. (e) S. Bahmanyar and K. N. Houk, *J. Am. Chem. Soc.* 2001, **123**, 12911; (f) C. E. Cannizzaro and K. N. Houk, *J. Am. Chem. Soc.* 2002, **124**, 7163.
16 R. C. Johnston, P. H.-Y. Cheong, *Org. Biomol. Chem.* 2013, **11**, 5057-5064.
17 Please see Electronic Supplementary Information (ESI).